Controlling tip vortices and cavitation with a grooved-tip design for tidal turbines

Yabin Liu, Junchen Tan, and Ignazio Maria Viola

Abstract—**Cavitation can result in blade erosion, vibration, and cavitation noise due to bubble collapse. Tidal turbines' blade tips experience the highest flow speed, and thus, risks of cavitation increase due to low pressure inside tip vortices at high Tip Speed Ratios (TSRs). This can cap their power efficiency and lead to an upper TSR limit. The present work focuses on controlling tip vortices through a novel approach: tip permeability achieved by a grooved tip design. A blade-resolved Reynolds-Averaged Navier-Stokes simulation has been carried out on a model-scale horizontal-axis turbine. In our work, the simulation results have been validated with existing experimental data from the UK Supergen Benchmarking turbine and our wing tip vortex measurements in a water tunnel. We modelled a porous zone placed over the blade tip section, demonstrating that there is an optimal permeability that can substantially reduce the tip vortex intensity and associated pressure drops, and thus mitigate the risk of cavitation. Building on this conclusion, in this study, we have developed a novel design with multiple grooves distributed along the blade tip chord, resulting in an equivalent local 2D permeability. The spanwise scope of the porous or grooved zone is 0.1% of the turbine diameter. It is found that the grooved tip design can significantly increase the minimum pressure coefficient at the tip vortex core by up to 27% at a TSR of 6. We also explored different groove channel designs, either by pitching the grooves or making them convergent. We found that, although the effects remain significant and relatively consistent across all design types, the tip vortices are most effectively suppressed when the groove channel has a convergent shape. This promising outcome suggests a substantial reduction of the tip vortex cavitation risks and can thus enable turbines to operate at higher TSRs. Additionally, as the spanwise extent of the permeable tip is minimal, the impact on the turbine's power and thrust coefficients is slight.**

Index Terms—**Tidal turbine, tip vortices, cavitation, grooved-tip, flow control**

Part of a special issue for EWTEC 2025. Original version published in EWTEC 2025 proceedings at doi.org/10.36688/ewtec-2025-759.

This paper has been subject to single-blind peer review by a minimum of two reviewers.

This work has been supported by the Royal Commission for the Exhibition of 1851 Brunel Fellowship, the UK, EPSRC funded, Supergen Offshore Renewable Energy Hub [EP/Y016297/1], the Royal Society ISPF-International Collaboration Award [ICA/R1/231053], the EPSRC IAA Innovation Competition [EPSRC IAA PV111], and the EPSRC-funded 'Morphing-Blades' project [EP/V009443/1].

Y.Liu and J.Tan are at Department of Engineering, King's College London, London, WC2R 2LS, UK (e-mail for correspondence: yabin.liu@kcl.ac.uk).

I.M.Viola is at School of Engineering, University of Edinburgh, Edinburgh, EH9 3BF, UK.

Digital Object Identifier: https://doi.org/10.36688/imej.9.65-71

I. Introduction

TIDAL power has the potential to play a significant role in the transition to net-zero energy. In the third quarter of 2024, onshore and offshore wind accounted for 26% of the total electricity generation in the United Kingdom, with hydroelectricity contributing an additional 2% [1]. Furthermore, tidal stream resources have the potential to generate 34 TWh per year - equivalent to 11% of the UK's current electricity demand [2]. However, both wind and tidal turbines face persistent challenges related to vortices and their associated wake [3, 4], cavitation [5, 6] and noise [7], which limit the efficiency and durability of the turbines. Tidal turbines, in particular, experience more severe erosion due to prolonged exposure to seawater [8], and their tips experience the highest flow velocity with a significantly increased risk of cavitation and cavitation-caused damage. Therefore, reducing the intensity of blade tip vortices and mitigating the cavitation risks will allow tidal turbines to operate at higher Tip Speed Ratios (TSRs) without compromising their reliability, ultimately increasing the amount of power that can be harvested.

Blade tip vortices form due to the pressure imbalances between the pressure and suction sides of a blade, creating highly vortical flow structures that lead to a pressure drop in the centre region. The two types of tip flow in turbomachinery, tip leakage vortices in the presence of a casing wall with a gap between the rotating blades and the casing wall, and tip vortices when there is no casing wall, share the same underlying flow physics. In underwater applications, such as ship propellers and tidal stream turbines, tip vortices are often linked to cavitation due to pressure drop within the vortex core [5, 9]. The intensity of tip vortices is often an indicator for the local pressure drop inside the vortex core [10, 11] as well as the vortex breakdown [12, 13], thus having a dominant influence on the cavitation risks, flow unsteadiness, and wake recovery.

To mitigate the tip (leakage) vortex intensity, Liu *et al.* [14] proposed a blade tip design incorporating a single groove, which showed a significant potential to suppress the tip leakage vortices and associated cavitation A micro jet is passively generated at the groove and interacts with the primary tip leakage vortex, producing a promising jet-induced vortex breakdown effect. However, a subsequent experimental study by Jiang *et al.* [15] revealed that the centralised jet flow may introduce new cavitation risks due to the high velocity inside the groove. Taking inspiration from

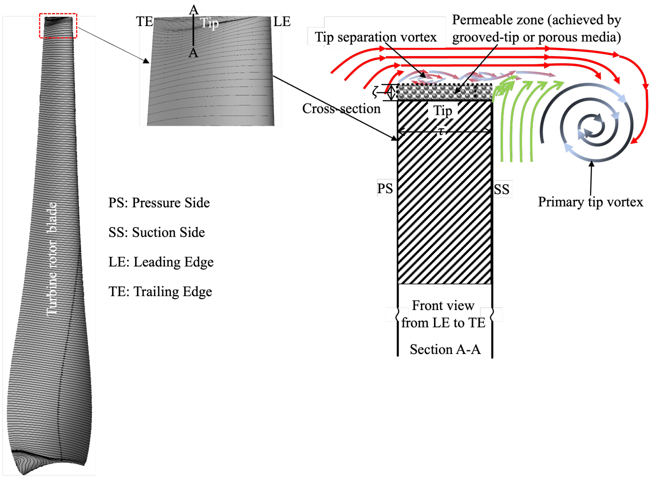

Fig. 1. Schematic of a permeable tip for a tidal turbine blade

nature, where permeability is often used to control vortical structures [16], we proposed a novel approach of permeable tip treatment [17] (as shown in Figure 1). Simulations of the model-scale tidal turbine used in UK Supergen ORE Tidal Benchmarking Project [18] showed the effects of imposing a uniform Darcy-type permeability at the blade tip region. Building on the promising results of these simulations, the present study presents a practical engineering solution: a multi-groove blade tip design that leverages uniform permeability in controlling wakes, while addressing the new cavitation risks identified by Jiang *et al.* [15] for the single groove approach.

Porous media have already been successfully used for controlling tip vortices, typically to mitigate noise in turbomachinery [19, 20]. Furthermore, a porous metal tip of a hydrofoil was found to mitigate the tip clearance cavitation generated by the vicinity of the tip to the side wall of a cavitation tunnel [21]. However, those experiments focused on the effects of tip gap sizes, while the specific role of permeability was not explained. Other studies showed that the tip vortex intensity can be modified by equipping the blade tip geometry with rounded tips [22], thickening and raking tips [23], and bionic wavy tips [24].

Here, we present a practical approach to reducing tip vortex intensity and minimising the associated cavitation risks by incorporating multiple grooves at the blade tips. Building on our previous work [17, 25], we employ blade-resolved Reynolds-Averaged Navier-Stokes (RANS) simulations to model a horizontal-axis tidal turbine with grooved-tip designs. The groove configurations are initially guided by porous media simulations in Liu *et al.* [17] to ensure similar local permeability characteristics. Subsequently, we assess their effectiveness in mitigating tip vortices and reducing pressure drops. We then analyse the pressure coefficient distribution and internal flow patterns within the grooves to gain insight into the underlying flow physics. Finally, we compare the turbine's power and thrust coefficients to evaluate the impact of grooved-tip designs on its overall energy performance.

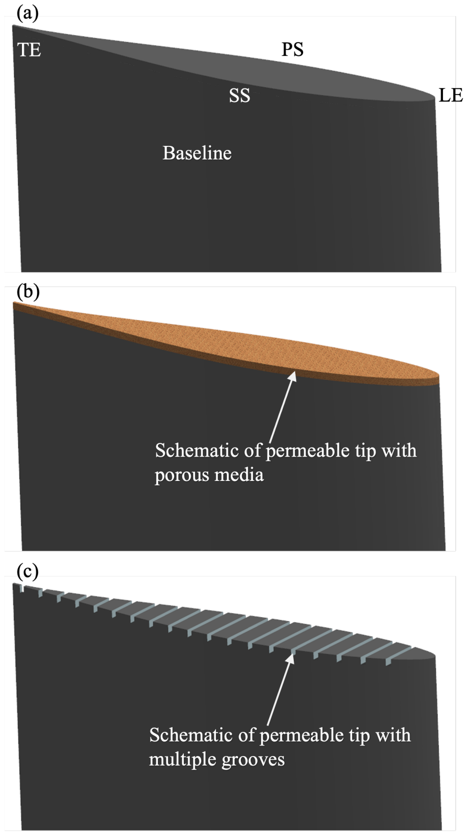

Fig. 2. Schematic of permeable tip treatment: (a) baseline blade without a permeable tip; (b) a permeable tip with porous media; (c) a permeable tip with multiple grooves

II. Methodology and Validation

A. Model and grooved-tip designs

In the present work, we develop a novel structure featuring multiple grooves to replicate the permeability effects modelled by porous media in our previous work [17]. A schematic of a permeable tip using porous material is shown in Figure 2b, while the design incorporating multiple grooves is depicted in Figure 2c.

As described in Appendix A, the chordwise dimension and number of grooves are determined based on a two-dimensional (2D) channel simulation, ensuring that the design with multiple grooves achieves a local 2D permeability similar to that of the porous media simulation. The design consists of 25 grooves oriented in the chord-normal direction, each with a width of 1% of the tip chord. Additionally, we explore three alternative designs Figure 3 by varying the contraction ratio and the direction from the pressure side (PS) and suction side (SS) for each groove. The spanwise extent of the groove structures is set to 0.1% of the rotor diameter, consistent with the porous media simulation by Liu *et al.* [17].

B. Numerical methods and validation

This study employs Computational Fluid Dynamics (CFD) simulations to analyse one-third of a tidal turbine rotor (Figure 4a) within a rotating, non-inertial reference frame within Ansys Fluent. Periodic conditions are enforced at the two inner side boundaries

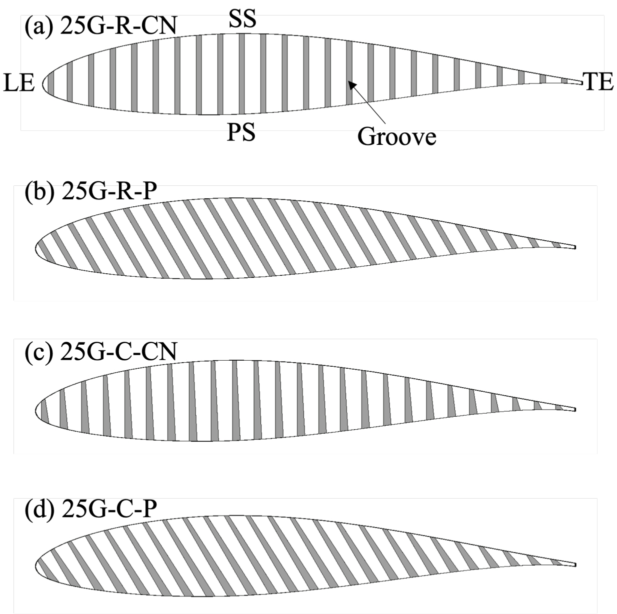

Fig. 3. Four types of groove designs: (a) 25G-R-CN: 25 rectangular, chord-normal grooves; (b) 25G-R-P: 25 rectangular, pitched (by 30°) grooves; (c) 25G-C-CN: 25 convergent (convergent ratio 2:1), chord-normal grooves (d) 25G-C-P: 25 convergent (convergent ratio 2:1), pitched (by 30°) grooves.

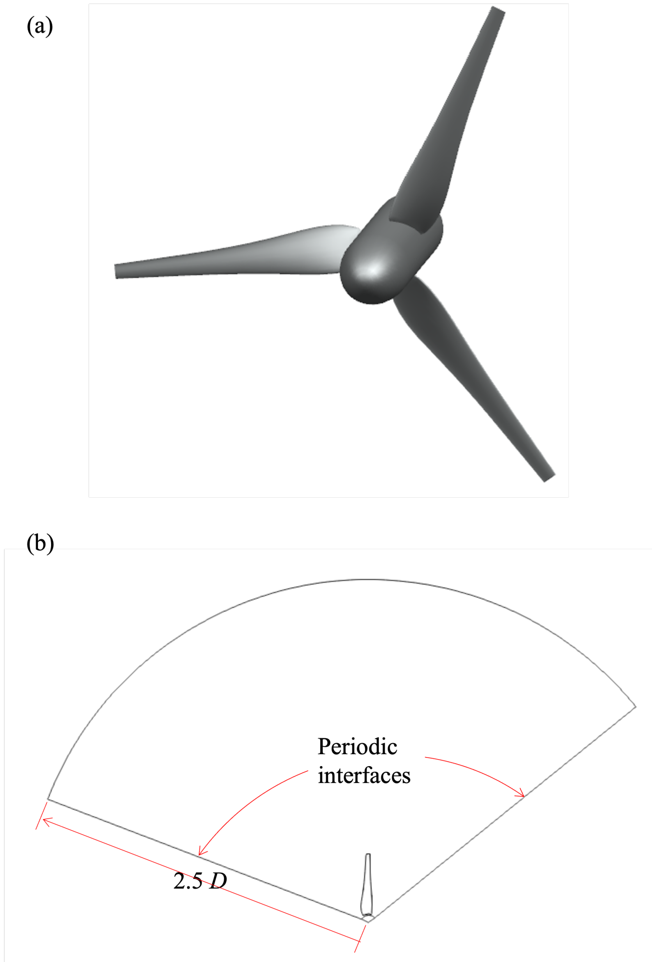

Fig. 4. Model: (a) turbine rotor with three blades (b) axial view of the 120°-wedge computational domain

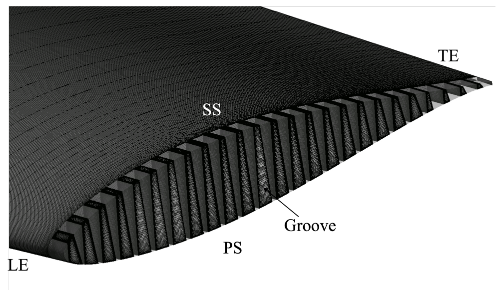

Fig. 5. Mesh on the turbine blade and grooves.

(Figure 4b). The horizontal-axis turbine, with a 1.6 m rotor diameter D, was tested by the UK Supergen Offshore Renewable Energy Hub [18]. Experimental data were obtained from towing tank tests conducted at a Reynolds number of 1.3×10^6, determined using a constant towing velocity of $U_\infty = 1$ ms^{-1} and the rotor diameter as the characteristic length.

The SST $k - \omega$ turbulence model is employed in the simulations. A uniform, constant free-stream velocity with low turbulence intensity, specified as 10^{-6}, is specified at the upstream inlet boundary. The downstream outlet boundary is assigned a constant zero pressure. A slip condition is applied at the outer boundary, while no-slip conditions are applied to the blade and hub surfaces. A non-conformal interface technique is employed to connect the rotor domain with the groove channel. The validation and verification of the employed numerical method have been performed in our previous work [17], which shows a good agreement between the simulation results and the experimental data.

The computational domain is discretised using ICEM-CFD, generating a structured mesh of approximately 33 million hexahedral cells for a case with multiple grooves. As shown in Figure 5, the mesh along the blade-tip chord direction is further refined (compared to the mesh used in Liu *et al.* [17]) to predict the flows going through the grooves accurately. The boundary layer of the blade and the groove walls is accurately resolved, maintaining an average y^+ around one at the design tip speed ratio of 6.03.

III. Results

A. Vortex pattern and pressure coefficient at the vortex cores

In Figure 6, we compare the 3D streamlines originating from the blade tip for the baseline case and the permeable tip designs featuring multiple grooves. The simulation results indicate that the grooved-tip design effectively mitigates tip vortex intensity and the associated pressure drops by significantly increasing the radial extent of the primary tip vortex and enhancing vortex diffusion. Furthermore, the presence of these grooves suppresses the tip separation vortex and displaces the primary tip vortex away from the blade suction surface, thereby further reducing the risk of blade damage in the event of cavitation within the vortex. These behaviours align with the permeability effects observed in porous media, as reported in Liu *et al.* [17].

Figure 7 illustrates the tip vortex structure, defined by the Q criterion, along with the pressure coefficient

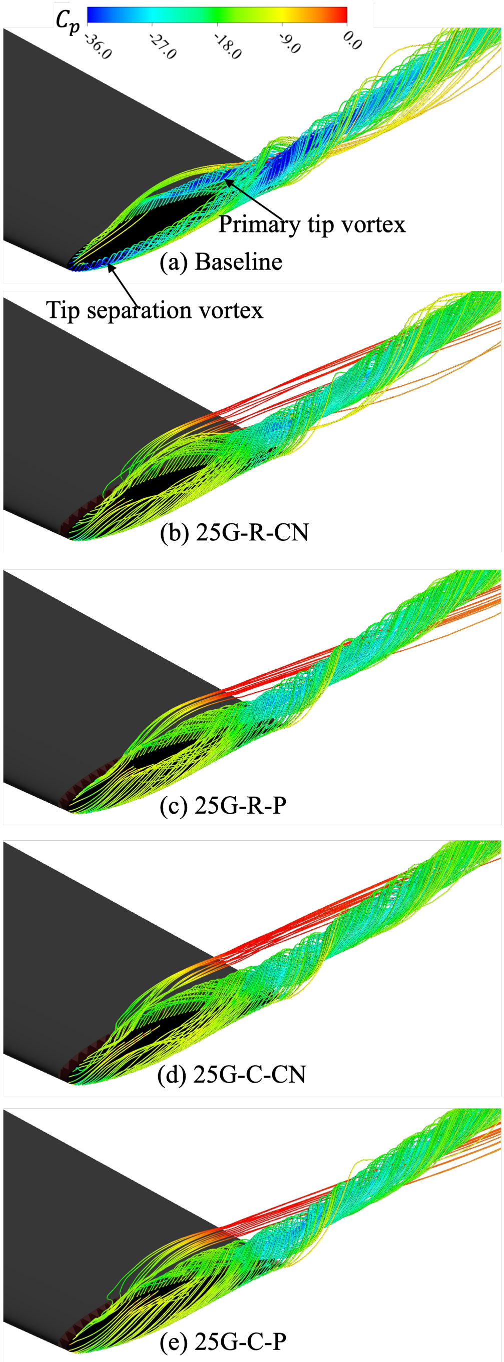

Fig. 6. Comparison of 3D streamlines released from the blade tip between: (a) Baseline; (b) 25G-R-CN; (c) 25G-R-P; (d) 25G-C-CN; (e) 25G-C-P. The pressure-coefficient C_p is defined as $C_p = \frac{p - p_\infty}{\frac{1}{2}\rho U_\infty^2}$, where p_∞ is the inlet pressure and U_∞ is the inflow freestream velocity (towing velocity in the experiment).

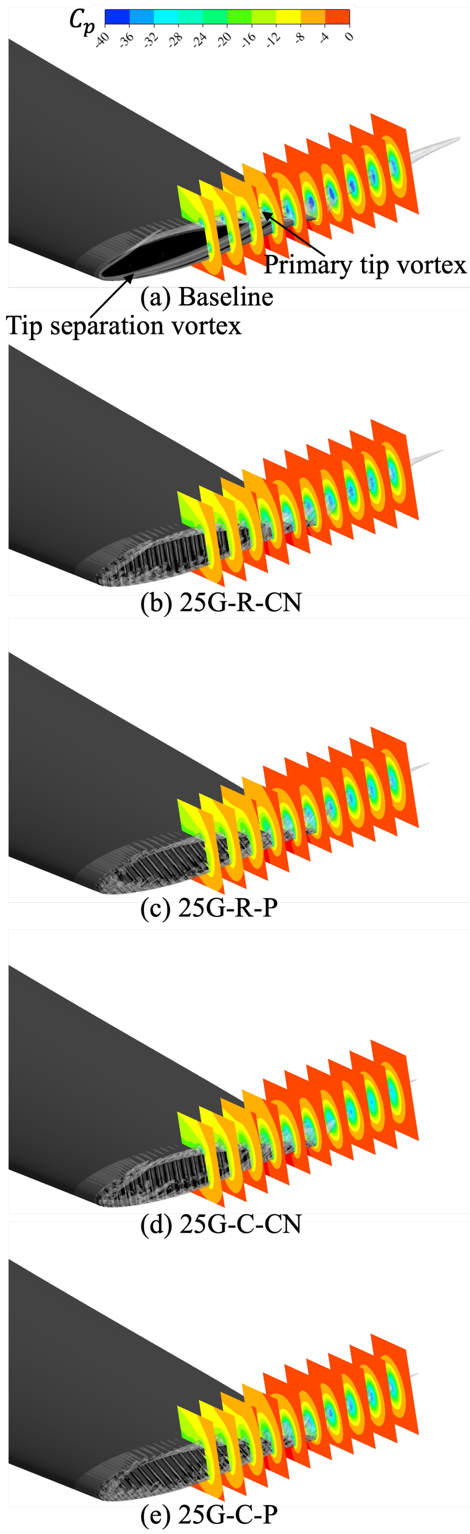

Fig. 7. Comparison of tip vortices visualised by Q criterion, where $QD^2/U_\infty^2 = 6.4 \times 10^6$, and distribution of pressure coefficient on cross-sections between: (a) Baseline; (b) 25G-R-CN; (c) 25G-R-P; (d) 25G-C-CN; (e) 25G-C-P.

(C_p) distribution across multiple cross-sections. These sections extend from the mid-chord position ($y/c = 0.5$) to the trailing edge ($y/c = 1.0$) and further into the wake region at $y/c = 1.4$. The grooved-tip designs significantly reduce the pressure drops associated with the primary tip vortex, particularly during its merger with the tip separation vortex near the trailing edge. Additionally, the tip vortices fragment into smaller structures due to the influence of the grooves and the jet flows generated within the groove channels.

We further quantitatively analyse the effects by extracting the minimal C_p on each cross-section along the primary tip vortex trajectory. As demonstrated in Figure 8, the grooved-tip designs effectively increase the minimal pressure coefficient within the primary tip vortex by up to 27%, significantly mitigating the risk of cavitation in a tidal turbine. Although all four types of grooved-tip designs demonstrate significant and consistent efficacy, the 25G-C-CN design exhibits

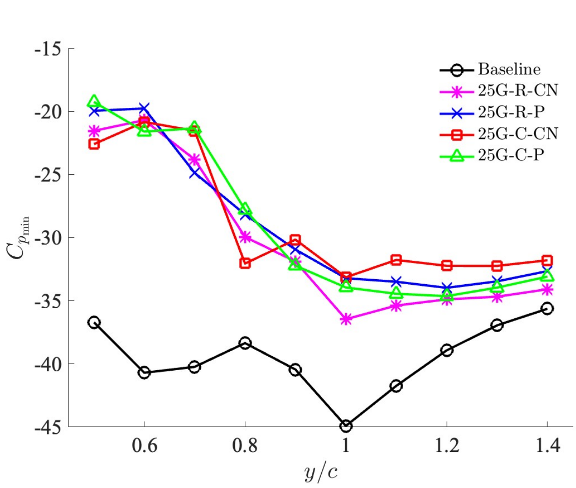

Fig. 8. Comparison of minimal pressure coefficient along the primary tip vortex trajectory.

the optimal effect, while the 25G-R-CN design shows the least effect overall.

B. *Pressure coefficient inside the grooves*

As highlighted by Jiang *et al.* [15], a potential drawback of the single-groove design proposed in Liu and Tan [14] is the risk of cavitation within the groove, caused by high flow velocity and the resulting local low pressure. To investigate this issue, we further analyse the pressure coefficient distribution along a circumferential cut through the multiple grooves in the present work, as shown in Figure 9. The results indicate that the multiple-groove design substantially mitigates this problem due to the lower flow speeds within the grooves, thereby reducing the risk of cavitation inside the groove channels. Although local low pressure occurs in several grooves, the scope of this phenomenon is very limited, and the extent of the pressure drop is moderate. Figure 9 also shows that the 25G-C-CN design demonstrates the optimal effect in reducing pressure drops in the primary tip vortex, particularly in the region near the trailing edge.

To understand the reason for the moderately superior effect demonstrated by the 25G-C-CN design, we present the velocity vectors inside and around the grooves along the same cut through the multiple grooves in Figure 10. It is evident that the 25G-C-CN design induces the strongest interaction between the jet flows from the groove channels and the primary tip vortex. In contrast, the 25G-R-CN design, which shows the weakest effect in Figure 8 among the four designs, generates a lower level of interaction due to the vortical flows formed inside the groove channels. This indicates that a practical design must consider both general effects, such as overall permeability, and local effects, such as the local blockage within the groove channels.

C. *Power and thrust performance*

In this section, we examine the impact of the grooved-tip design on the turbine's power coefficient

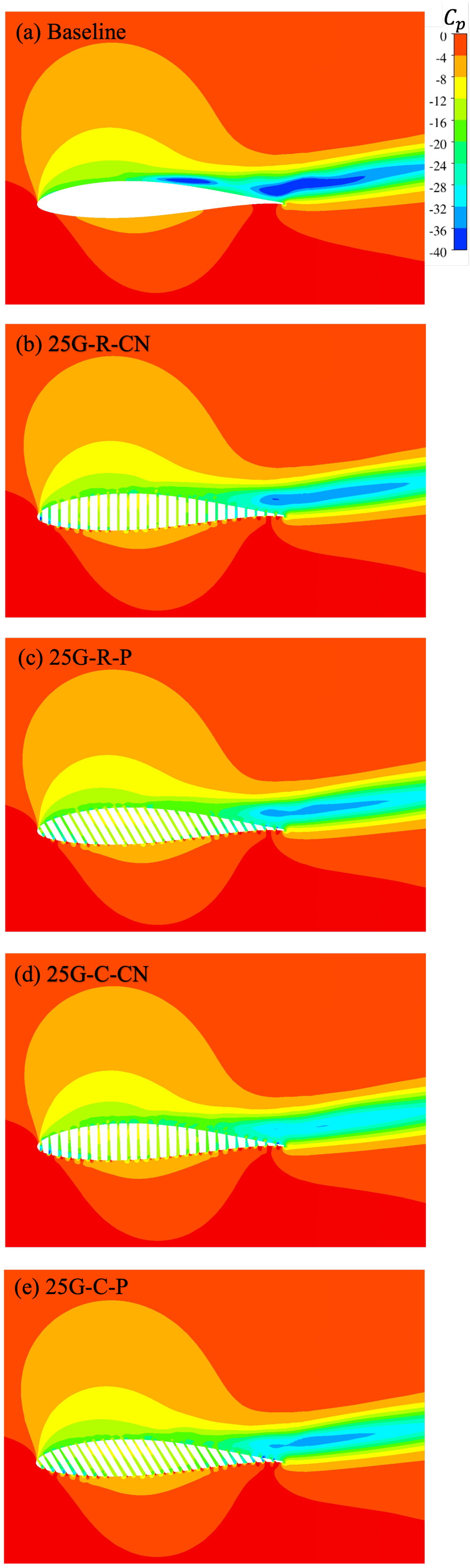

Fig. 9. Distribution of pressure coefficient on a circumferential section at 99.825% radius of the turbine rotor: (a) Baseline; (b) 25G-R-CN; (c) 25G-R-P; (d) 25G-C-CN; (e) 25G-C-P.

(C_P) and thrust coefficient (C_T). Given that the spanwise extent of the groove structures is only 0.1% of the turbine diameter—approximately 0.23% of the turbine blade's radial length—the influence of the grooved-tip designs is minimal across all configurations. As shown

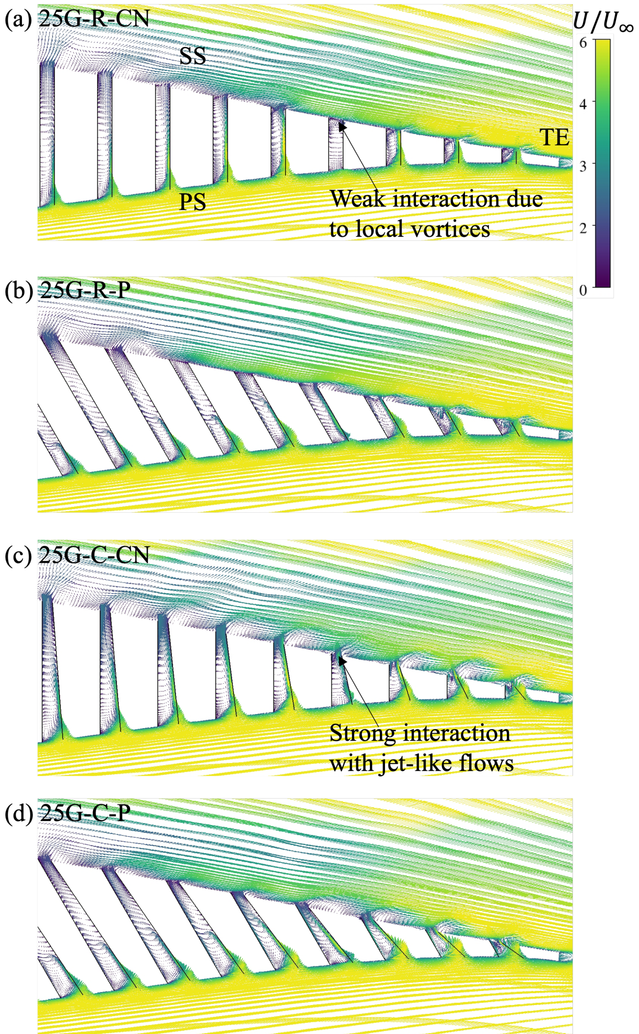

Fig. 10. Velocity vector inside and around the grooves on a circumferential section at 99.825% radius of the turbine rotor: (a) 25G-R-CN; (b) 25G-R-P; (c) 25G-C-CN; (d) 25G-C-P.

TABLE I
COMPARISON OF POWER AND THRUST COEFFICIENTS AMONG DIFFERENT GROOVED-TIP DESIGNS

Design Type	25G-R-CN	25G-R-P	25G-C-CN	25G-C-P
$C_P/C_{P_{\text{Baseline}}}$	0.9915	1.0018	0.9993	1.0243
$C_T/C_{T_{\text{Baseline}}}$	0.9918	1.0002	1.0017	1.0156

in Table I, the relative change in C_P ranges from -0.85% to 2.43% compared to the baseline case, while the relative change in C_T ranges from -0.82% to 1.56%.

IV. Conclusion and Discussion

In the present work, we introduce an innovative method to reduce tip vortex intensity and the associated cavitation risks by incorporating tip permeability through a grooved tip design for tidal turbines. This builds upon our previous work, which demonstrated that the permeable tip treatment with optimised permeability can significantly lower tip vortex intensity and pressure drops, thereby mitigating the risk of cavitation.

Using blade-resolved RANS simulations, we have developed a novel grooved-tip design that replicates the local 2D permeability effect. Our findings show that the grooved-tip design significantly enhances the minimum pressure coefficient at the tip vortex core, with an increase of up to 27% at a tip speed ratio of six. Additionally, we explore various groove configurations, including pitched and convergent designs, and discover that while all designs had consistent effects, the convergent groove design proved to be the most effective in suppressing the tip vortices and associated pressure drops.

Additionally, the minimal spanwise extent (0.1% of the turbine rotor diameter) of the grooved tip ensures a slight impact on the turbine's power and thrust coefficients, with a relative change in C_P of up to 2.43% and a relative change in C_T of up to 1.56%.

These findings underscore the effectiveness of the grooved-tip design in significantly reducing cavitation risks, enabling turbines to operate at higher tip speed ratios while maintaining structural integrity. In general, this approach offers a highly efficient and practical solution for improving the performance and durability of tidal turbines, as well as other wing- or blade-based systems operating in underwater environments.

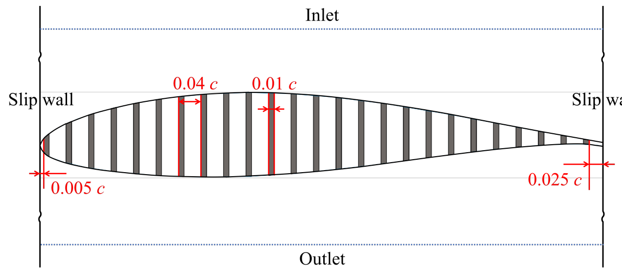

Fig. 11. Schematic of a permeable tip for a tidal turbine blade

Appendix A
2D Channel Simulation for Permeability Estimation

To guide the practical design of multiple grooves, a 2D channel simulation is conducted. As illustrated in Figure 11, the 2D channel includes a foil with the same profile as the turbine blade tip. Simulations are performed for two cases: (i) the foil is filled with a porous material of uniform permeability, characterised by the non-dimensional Darcy number Da (refer to [17] for the detailed definition of Da); (ii) the foil contains multiple grooves allowing flow passage, while the remaining region remains solid. When the pressure loss across the foil, defined as the pressure difference between the channel inlet and outlet boundaries, is identical in both cases, the groove configuration achieves the same 2D permeability (along the chord-normal direction). Given that the optimal permeability range has been identified as $Da = 10^{-6}$ to $Da = 10^{-5}$ [17], the corresponding groove configurations have been determined to fall in this range of permeability.

Acknowledgement

This work has been supported by the Royal Commission for the Exhibition of 1851 Brunel Fellowship, the UK, EPSRC funded, Supergen Offshore Renewable Energy Hub [EP/Y016297/1], the Royal Society ISPF-International Collaboration Award [ICA/R1/231053], the EPSRC IAA Innovation Competition [EPSRC IAA PV111], and the EPSRC-funded 'Morphing-Blades' project [EP/V009443/1].

References

[1] W. Spry, "Section 6: Renewables," in *Energy Trends: December 2024*. London: Department for Energy Security & New Zero, 2024, available at https://www.gov.uk/government/statistics/energy-trends-december-2024. Accessed: 2025-03-03.

[2] D. Coles, A. Angeloudis, Greaves *et al.*, "A review of the uk and british channel islands practical tidal stream energy resource," *Proceedings of the Royal Society A*, vol. 477, no. 2255, p. 20210469, 2021.

[3] L. Lignarolo, D. Ragni, F. Scarano, C. S. Ferreira, and G. Van Bussel, "Tip-vortex instability and turbulent mixing in wind-turbine wakes," *Journal of Fluid Mechanics*, vol. 781, pp. 467–493, 2015.

[4] A. Posa, R. Broglia, and E. Balaras, "Instability of the tip vortices shed by an axial-flow turbine in uniform flow," *Journal of Fluid Mechanics*, vol. 920, p. A19, 2021.

[5] Y. Liu, L. Tan, and B. Wang, "A review of tip clearance in propeller, pump and turbine," *Energies*, vol. 11, no. 9, p. 2202, 2018.

[6] A. Wimshurst, C. Vogel, and R. Willden, "Cavitation limits on tidal turbine performance," *Ocean Engineering*, vol. 152, pp. 223–233, 2018.

[7] R. C. Ramachandran, G. Raman, and R. P. Dougherty, "Wind turbine noise measurement using a compact microphone array with advanced deconvolution algorithms," *Journal of Sound and Vibration*, vol. 333, no. 14, pp. 3058–3080, 2014.

[8] G. Hou, X. Zhao, H. Zhou, J. Lu, Y. An, J. Chen, and J. Yang, "Cavitation erosion of several oxy-fuel sprayed coatings tested in deionized water and artificial seawater," *Wear*, vol. 311, no. 1-2, pp. 81–92, 2014.

[9] F. Pereira, F. Salvatore, and F. Di Felice, "Measurement and modeling of propeller cavitation in uniform inflow," *Journal of Fluids Engineering*, vol. 126, no. 4, pp. 671–679, 2004.

[10] Q. Ye, Y. Wang, and X. Shao, "Dynamics of cavitating tip vortex," *Journal of Fluid Mechanics*, vol. 967, p. A30, 2023.

[11] M. Dreyer, J. Decaix, C. Münch-Alligné, and M. Farhat, "Mind the gap: a new insight into the tip leakage vortex using stereo-piv," *Experiments in Fluids*, vol. 55, pp. 1–13, 2014.

[12] A. Posa, I. M. Viola, and R. Broglia, "Influence of the tip speed ratio on the wake dynamics and recovery of axial-flow turbines," *Physics of Fluids*, vol. 36, no. 5, 2024.

[13] Y. Liu, Z.-N. Wang, L. Tan, P. G. Tucker, and F. M. Möller, "Tip-leakage-flow excited unsteadiness and associated control," *Physics of Fluids*, vol. 36, no. 5, 2024.

[14] Y. Liu and L. Tan, "Method of c groove on vortex suppression and energy performance improvement for a naca0009 hydrofoil with tip clearance in tidal energy," *Energy*, vol. 155, pp. 448–461, 2018.

[15] J.-W. Jiang, C.-M. Xie, L.-H. Xu, L. Li, and W.-X. Huang, "The groove at blade tip designed for suppression of tip-leakage vortex may bring the risk of inducing new cavitation," *Physics of Fluids*, vol. 34, no. 12, 2022.

[16] C. Cummins, M. Seale, A. Macente, D. Certini, E. Mastropaolo, I. M. Viola, and N. Nakayama, "A separated vortex ring underlies the flight of the dandelion," *Nature*, vol. 562, no. 7727, pp. 414–418, 2018.

[17] Y. Liu, J. Tan, R. H. Willden, P. G. Tucker, and I. M. Viola, "Controlling tip vortices and cavitation through tip permeability for tidal turbines," *arXiv preprint arXiv:2408.16418*, 2024.

[18] R. Willden, X. Chen, S. Harvey, H. Edwards, C. Vogel, K. Bhavsar, T. Allsop, J. Gilbert, H. Mullings, M. Ghobrial *et al.*, "Tidal turbine benchmarking project: Stage i-steady flow blind predictions," National Renewable Energy Laboratory (NREL), Golden, CO (United States), Tech. Rep., 2023.

[19] M. R. Khorrami, F. Li, and M. Choudhari, "Novel approach for reducing rotor tip-clearance-induced noise in turbofan engines," *AIAA Journal*, vol. 40, no. 8, pp. 1518–1528, 2002.

[20] S. Palleja-Cabre, I. Saraceno, C. C. Paruchuri, and P. Joseph, "Reduction of tip-leakage noise by using porosity," in *28th AIAA/CEAS Aeroacoustics 2022 Conference*, 2022, p. 3061.

[21] Z. Bi, F. Bao, L. Zhang, X. Shao, and S. Li, "Numerical study of porous tip treatment in suppressing tip clearance vortices in cavitating flow," *Physics of Fluids*, vol. 36, no. 4, 2024.

[22] Q. Guo, L. Zhou, and Z. Wang, "Numerical evaluation of the clearance geometries effect on the flow field and performance of a hydrofoil," *Renewable Energy*, vol. 99, pp. 390–397, 2016.

[23] X. Q. Ji, X. Q. Dong, and C. J. Yang, "Attenuation of the tip-clearance flow in a pump-jet propulsor by thickening and raking the tips of rotor blades: A numerical study," *Applied Ocean Research*, vol. 112, p. 102723, 2021.

[24] L. Wang, X. Luo, J. Feng, J. Lu, G. Zhu, and W. Wang, "Method of bionic wavy tip on vortex and cavitation suppression of a hydrofoil in tidal energy," *Ocean Engineering*, vol. 278, p. 114499, 2023.

[25] Y. Liu, S. Gambuzza, R. Broglia, A. Young, E. McCarthy, and I. M. Viola, "On the accuracy of bemt and cfd on the power and trust prediction of tidal turbines," in *The 15th European Wave and Tidal Energy Conference*, 2023.